

The structure of $(\text{CH}_3)_3\text{SI}_3$. Comparison between the structure in the solid and liquid state

L.A. Bengtsson* and Å. Oskarsson

Inorganic Chemistry 1, University of Lund, PO Box 124, S-221 00 Lund (Sweden)

H. Stegemann*

Institut für Anorganische Chemie, FR Chemie, Ernst-Moritz-Arndt-Universität Greifswald, Soldtmannstrasse 16, D-17489 Greifswald (Germany)

A. Redeker

Physikalisches Institut der Universität Bonn, Nussallee 12, D-50939 Bonn (Germany)

(Received July 6, 1993)

Abstract

The crystal structure of $\text{Me}_3\text{SI}_3(\text{s})$ has been determined. The compound is monoclinic and crystallizes in the space group Cc (No. 9) with unit cell parameters $a=7.856(2)$, $b=17.733(6)$, $c=8.259(2)$ Å, $\beta=111.14(2)^\circ$, $U=1073(1)$ Å³ and $Z=4$. The structure contains pyramidal Me_3S^+ cations and almost centrosymmetric I_3^- anions. The near- $D_{\infty h}$ symmetry of the triiodides is verified by Raman spectroscopy, revealing one single peak at 110 cm^{-1} . The local structure of $\text{Me}_3\text{SI}_3(1)$ at 50°C and the sulfonium–triiodide coordination mode, as characterized by liquid X-ray scattering and Raman spectroscopy, is almost identical to that in the corresponding solid and the analogous Et_3SI_3 melt. The difference in sulfonium hydrocarbon chains induces very minor changes in the local structure of the trialkylsulfonium triiodides both in the solid and molten state. X-ray absorption spectroscopy, XANES, of the S-K edge reveals electronically identical sulfur atoms in solid and liquid triiodides, which also implies a similar local structure.

Key words: Crystal structures, Triiodide complexes; Alkyl sulfonium complexes

Introduction

A large number of triiodide crystal structures have been reported in recent years. There are examples of triiodides with simple inorganic cations, $\text{KI}_3 \cdot \text{H}_2\text{O}$ [1], complex cations, $[(\text{C}_5\text{H}_5)_2\text{Fe}]\text{I}_3$ [2], onium cations, $\text{N}(\text{C}_2\text{H}_5)_4\text{I}_3$ [3], and also of organic compounds such as $\text{C}_6\text{H}_5\text{CONH}_2 \cdot \text{HI}_3$ [4] and substituted pyridinium triiodides [5]. In particular, tetraalkyl and -aryl triiodide structures have been characterized. The triiodides of other onium cations of the fifth main group are also known, e.g. $[\text{PPh}_4]\text{I}_3$ [6] and $[\text{AsPh}_4]\text{I}_3$ [7].

However, knowledge about the fundamental and structural chemistry of sulfonium triiodides in particular and polyiodides in general is very limited. Even the crystal structure of the most simple polyiodide, Me_3SI_3 , is so far unknown. The structure of Me_3SI was characterized by Zuccaro and McCullough already in 1959

[8]. In previous work we have prepared and structurally investigated the physical properties and structure of various trialkyl sulfonium polyiodides. Me_3SI_3 forms a deep-red crystalline solid at room temperature (m.p. 37°C), but the corresponding triethyl compound is a liquid (m.p. -2°C) [9, 10]. Due to the low melting points of these compounds, the idea to compare the solid and liquid structures of Me_3SI_3 emerged. Such comparisons may provide further information about the I_3^- bond flexibility and sulfonium–triiodide coordination and interaction. The structure of $\text{Et}_3\text{SI}_3(1)$ was determined using Raman spectroscopy and liquid X-ray scattering [10], and was shown to consist of discrete triethylsulfonium and linear, centrosymmetric triiodide ions. The sulfonium–triiodide coordination is asymmetric. However, the orientation of the hydrocarbon chains could not be evaluated.

In this work, Me_3SI_3 has been synthesized and its crystal structure at room temperature and liquid structure at 50°C has been determined by means of Raman

*Authors to whom correspondence should be addressed

spectroscopy and X-ray diffraction. Comparisons between the solid and liquid structure of Me_3SI_3 and Et_3SI_3 and relevant literature data are made. The extent of interaction between the sulfonium cations and triiodides is estimated by means of X-ray absorption spectroscopy (XANES) data for various similar sulfur-containing compounds, which monitor the electronic sulfur environment.

Experimental

Chemicals

Trimethylsulfonium triiodide, Me_3SI_3 , was prepared by reaction of iodine and trimethylsulfonium iodide (Riedel-de-Haen) in equimolar ratio in an ethanol solution. Single crystals were grown in ethanol at -15°C as thin red–yellow plates.

Crystal structure determination

A crystal of Me_3SI_3 with the approximate dimensions $0.375 \times 0.250 \times 0.050$ mm was used in the crystal structure analysis. The crystal was stable over the time of experiment. All measurements were performed on an Enraf-Nonius CAD-4 diffractometer with graphite-monochromatized $\text{Mo K}\alpha$ radiation.

Cell constants and orientation matrix for data collection were obtained from a least-squares refinement using the setting angles of 45 carefully centred reflections in the range $12.17 < 2\theta < 31.38^\circ$. The Laue class is $2/m$ and the space group is Cc (No. 9), which was determined from the systematic absence of $hkl: h+l \neq 2n$ and $h0l: l \neq 2n$, statistical analysis of the intensity distribution, packing considerations and the successful solution and refinement of the structure. The values of I and $\sigma(I)$ were corrected for Lorentz, polarization and absorption effects, the latter by numerical integration. Unit cell data and experimental details are summarized in Table 1 and atom coordinates in Table 2. The fairly large temperature factors reflect that the intensity data were collected only $c. 15^\circ\text{C}$ below the melting point.

Liquid X-ray scattering

The liquid structure of the Me_3SI_3 melt was investigated at 50°C . The melt was kept in a Teflon container inside a furnace with a closed compartment and a 0.01 mm Al window. The furnace has been described elsewhere [11, 12]. The scattered radiation from the surface of the melt was detected at discrete angles between $1.2 < 2\theta < 108.4^\circ$. The measurements were performed on a Seifert GSD θ – θ diffractometer using $\text{Mo K}\alpha$ radiation. The scattered radiation was detected with a EG&G ORTEC Germanium solid state detector, in which the photon energy discrimination was electron-

TABLE 1 Unit cell parameters and experimental crystal data of $\text{Me}_3\text{SI}_3(\text{s})^a$

Formula	$\text{C}_3\text{H}_9\text{I}_3\text{S}$
M (g mol^{-1})	457.88
Crystal group	monoclinic
Space group	Cc (No. 9)
Laue symmetry	$2/m$
a (\AA)	7.856(2)
b (\AA)	17.733(6)
c (\AA)	8.259(2)
β ($^\circ$)	111.14(2)
U (\AA^3)	1073(1)
Z	4
D_c (g cm^{-3})	2.834
Temperature ($^\circ\text{C}$)	23
$F(000)$	808
Radiation (graphite monochromator)	$\text{Mo K}\alpha$, 0.7107 (\AA)
μ (cm^{-1})	87.65
Maximal 2θ ($^\circ$)	56.0
No. unique reflections	2662
No. reflections with $I > 3\sigma(I)$	765
Variation of two standard reflections (%)	± 2
Range of transmission factors	0.17–0.58
Method of refinement	full-matrix least-squares
Anomalous dispersion	all non-hydrogen atoms
No. of variables	63
R	0.056
R_w	0.084

^aThe structure was solved by direct methods. All computations were performed with Texsan Structure Analysis Software, MSC, 3200 Research Forest Drive, The Woodlands, TX 77381, USA.

TABLE 2 Fractional coordinates and isotropic thermal parameters of Me_3SI_3

Atom	x/a	y/b	z/c	B_{eq}^a
I1	0.5500	0.3207(2)	0.0200	6.1(2)
I2	0.4440(5)	0.1774(2)	0.1374(6)	4.7(1)
I3	0.3359(6)	0.0371(2)	0.2571(6)	5.5(1)
S	0.742(2)	0.0965(5)	0.888(1)	4.5(1)
C1	0.933(6)	0.166(2)	0.986(6)	6(2)
C2	0.596(7)	0.150(3)	0.695(7)	6(2)
C3	0.86(1)	0.030(3)	0.799(9)	10(3)

^a $B_{\text{eq}} = (8\pi^2/3) \sum_{i=1}^3 \sum_{j=1}^3 (U_{ij} a_i^* a_j^* a_i a_j)$.

ically adjusted. The low maximum value of 2θ is due to the experimental setup, in which a heating element above the surface of the melt cuts off incident and scattered radiation at high θ values. As a consequence, the shorter atom–atom distances are slightly affected in the Fourier transform. This subject will be briefly addressed in the discussion (*vide infra*). Corrections were made for Compton scattering, polarization and background radiation. The data treatment has been described in detail previously [12]. The composition and physical data of the Me_3SI_3 melt are given in Table 3.

TABLE 3 Composition and physical data of $\text{Me}_3\text{SI}_3(\text{l})$

C_I^a	C_S^a	C_C^a	C_H^a	V^b (\AA^3)	ρ (g cm^{-3})	μ (cm^{-1})
16.94	5.65	16.94	50.83	98.0	2.586	82

^aConcentrations in mol dm^{-3} . ^bPer iodide atom

Raman spectroscopy

The backscattering from the $\text{Me}_3\text{SI}_3(\text{s})$, $\text{Et}_3\text{SI}_3(\text{l})$ (room temperature) and $\text{Me}_3\text{SI}_3(\text{l})$ (50 °C) samples were recorded using the 1064 nm radiation of a low-power Nd:YAG laser in a Bruker IFS-66/FRA-106 FT Raman spectrometer with a germanium-diode detector. The resolution used was 4 cm^{-1} .

X-ray absorption spectroscopy, XANES

The XANES spectra were recorded at the beamlines BN2 and BN3 using synchrotron radiation of the Electron Stretcher Accelerator, ELSA in Bonn, operating in storage mode at 1.9 GeV and with an average current of about 50 mA [13]. The X-ray beam is monochromatized by a double-crystal X-ray monochromator of Lemmonier type equipped with two InSb(111) crystals [14]. Such crystals have a $2d$ of 7.4806 \AA and a resolution of 0.8 eV at the S-K edge. The monochromatic photon flux rate was about 10^9 photons per second and per energy interval. The monochromatized beams were passed through a reference ionization chamber, a sample chamber and finally through the detector ionization chamber. The absorption of air was minimized by reducing the pressure in the ionization chambers to 60 mbar. In this way the transmitted intensity was optimized. The logarithm of the ratio of the currents in the reference and detector chambers as a function of the energy of the incident radiation gives the absorption cross section. The photon energy was scanned from 2450 to 2510 eV in steps of 0.03 eV and with an integration time of 0.2 s per step. The experimental setup was calibrated to the maximum absorption at the S-K edge of ZnSO_4 (2481.44 eV). This compound was chosen as an energy standard due to its high stability. The calibration could be reproduced to within 0.05 eV .

Results and discussion

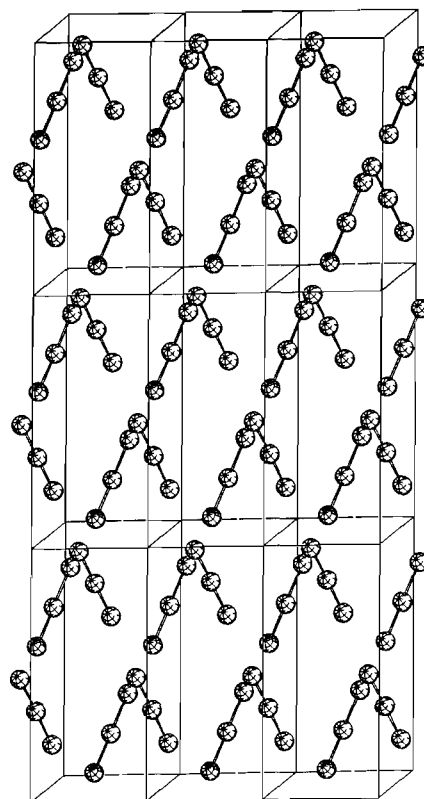
Crystal structure of $\text{Me}_3\text{SI}_3(\text{s})$

The unit cell of $\text{Me}_3\text{SI}_3(\text{s})$ contains discrete, almost centrosymmetric I_3^- and pyramidal Me_3S^+ ions. The triiodide deviates only slightly from perfect $D_{\infty h}$ symmetry; the central angle is 179° and the two short iodine-iodine distances are 2.915 and 2.946 \AA , respectively. These values correspond well to those observed for other triiodides (Table 4).

TABLE 4 Triiodide structural parameters of some solid triiodide compounds. The e.s.d.s amount to one or a few units in the last decimal cited

Compound	I-I (\AA)	(I-I-I) ($^\circ$)	Ref	
$[\text{Ph}_4\text{As}]\text{I}_3$	2.919	2.919	174.7	7
$[\text{Et}_4\text{N}]\text{I}_3$	2.928	2.928	180.0	3
$[\text{Et}_4\text{N}]\text{I}_3$	2.943	2.943	180.0	3
$\text{KI}_3 \cdot \text{H}_2\text{O}$	2.925	2.935	178.8	1
$[\text{H}_4\text{N}]\text{I}_3$	2.791	3.113	178.6	15
CsI_3	2.842	3.038	178.0	7
$[\text{UrH}]\text{I}_3^a$	2.923	2.941	178.3	16
$[\text{UrEt}]\text{I}_3$	2.906	2.906	180.0	16
$[\text{UrBu}]\text{I}_3$	2.889	2.935	179.1	16
$[\text{Bu}_4\text{N}]\text{I}_3$	2.887	2.951	178.4	4
	2.910	2.941	174.7	
$(\text{Benz})_2 \cdot \text{HI}_3^b$	2.924	2.934	178.0	4
	2.935	2.939	176.9	
$[\text{PyEt}]\text{I}_3^c$	2.906	2.936	177.7	5
$[\text{PyMe}_3]\text{I}_3$	2.907	2.929	179.8	5
$[\text{Ni}(\text{NH}_3)_6][(\text{I}_3)_2]$	2.923	2.923	180.0	17
	2.917	2.917	177.7	

^aUr = urotropinium. ^bBenz = benzamide ^cPy = pyridinium

Fig. 1 Orientation of triiodide ions in crystalline Me_3SI_3 .

The shortest $\text{I}_3^- - \text{I}_3^-$ distance is 4.334 \AA which is almost equal to twice the van der Waal's radius, 4.4 \AA , of iodine. Only very weak covalent interaction should

thus be expected. The I_3^- ions are arranged in two differently oriented piles of triiodides (Fig. 1). In the bc plane the ions form a pattern like foot tracks (Fig. 2). The M_3S^+ cation is positioned between the two piles. The cation has a pyramidal structure (Fig. 3).

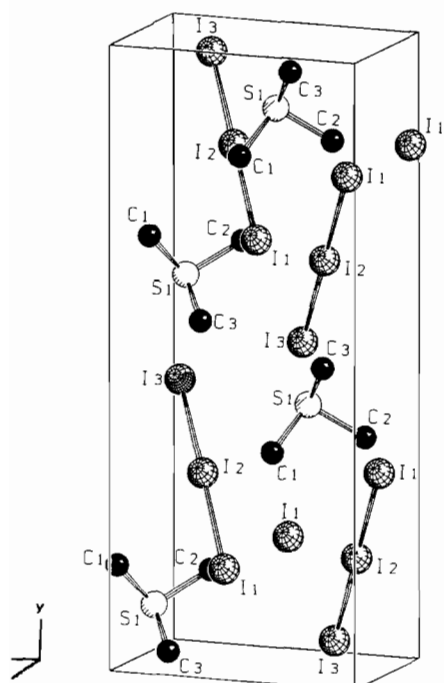
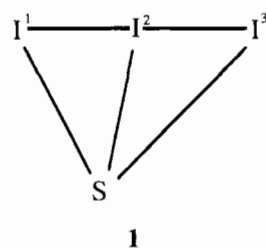


Fig. 2. The crystallographic unit cell of Me_3SI_3 .

Analogous to the ammonia molecule the C-S-C angles are smaller than a perfect tetrahedral angle, 99–103°. Packing effects and possibly weak interactions with the triiodide ions make both S-C distances and C-S-C angles slightly unequal (Table 5). The S-C distances in Me_3SI_3 are on average slightly longer than those reported for the corresponding Me_3SI compound [8].

The I-S distances and the sulfonium-triiodide coordination mode in $Me_3SI_3(s)$ are of special interest, since they agree with the coordination model proposed for liquid Et_3SI_3 and $Me_3SI_3(1)$. Theoretical calculations on the interaction between Br_3^- and K^+ reveal an energy minimum for an analogous coordination mode [18]. Note the different notations used below, where the symbols I^1, I^2, I^3 refer to the coordination model 1, and $I1, I2, I3$ refer to the crystallographic atoms defined in Table 2.



The S-I distances are 4.05, 4.57 and 5.17 Å in the structure model suggested for $Et_3SI_3(l)$. No information about the orientation of the hydrocarbon chains could

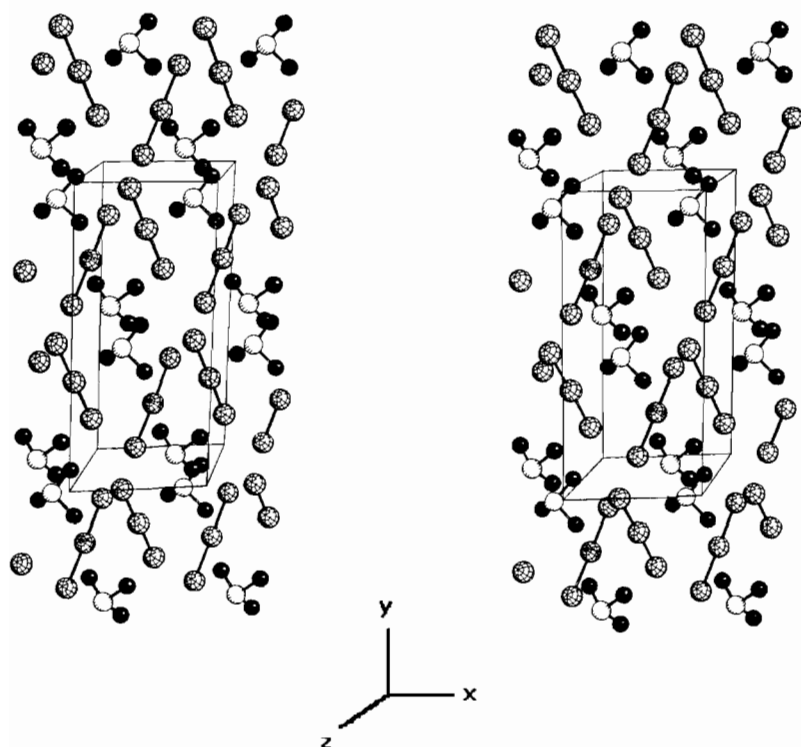


Fig. 3. A stereoscopic view of the crystal structure of Me_3SI_3 .

TABLE 5. Intramolecular distances and angles in $\text{Me}_3\text{SI}_3(\text{s})$

Interaction	Distance (Å)
I1-I2	2.946(4)
I2-I3	2.915(4)
S-C1	1.88(4)
S-C2	1.85(5)
S-C3	1.80(5)
	Angle (°)
I1-I2-I3	179.0(1)
C1-S-C2	101(2)
C1-S-C3	99(3)
C2-S-C3	103(3)

be distinguished; probably for dynamic reasons. The shortest S-I distances in solid Me_3SI_3 are S-I3 = 3.81, S-I2 = 3.91 and S-I1 = 4.52 Å. However, due to the coordination of the sulfonium ions to two triiodides in the solid structure, the shortest distance is to one triiodide ion and the other two to another. The position of the sulfur atom is, with respect to the triiodides, analogous to that shown in **1**. The corresponding I-S distances to a single triiodide are S-I3 = 5.25, S-I2 = 3.91 and S-I1 = 4.52 Å. In analogy to the coordination mode of a water molecule to anions, with the hydrogens in the direction of the negative charge, it was expected that the hydrocarbon chains would point towards the triiodides. However, in solid Me_3SI_3 both the hydrocarbon end and the end of the free electron pair are directed towards neighbour triiodides. The shortest I-S distance in the corresponding monoiodide, Me_3SI , is 3.95 Å [8].

Liquid structure of $\text{Me}_3\text{SI}_3(\text{l})$

The reduced intensity function and reduced radial distribution function (rRDF) of $\text{Me}_3\text{SI}_3(\text{l})$ at 50 °C are shown in Fig. 4. The rRDF is almost identical to that obtained at room temperature for $\text{Et}_3\text{SI}_3(\text{l})$ (Fig. 5). The strong peaks at 2.91 and 5.86 Å correspond to the I¹⁻³-I² and I¹⁻³-I³ distances (**1**) in the triiodide ion and are the same as in many crystalline triiodides (Table 4). In the region 0–6 Å there is only one significant difference; the peak at 2.9 Å appears to be lower and wider in the Me_3SI_3 melt than in $\text{Et}_3\text{SI}_3(\text{l})$. This effect is artificial and due to the data treatment. Since only data up to $s_{\text{max}} = 14.0 \text{ \AA}^{-1}$ could be used in the Fourier transform for the methyl compound, as compared to 15.0 \AA^{-1} for the ethyl compound, the short-distance peaks become slightly suppressed. The rRDFs indicate that the structure in both melts is fully analogous and consists of R_3S^+ ions and linear, centrosymmetric I_3^-

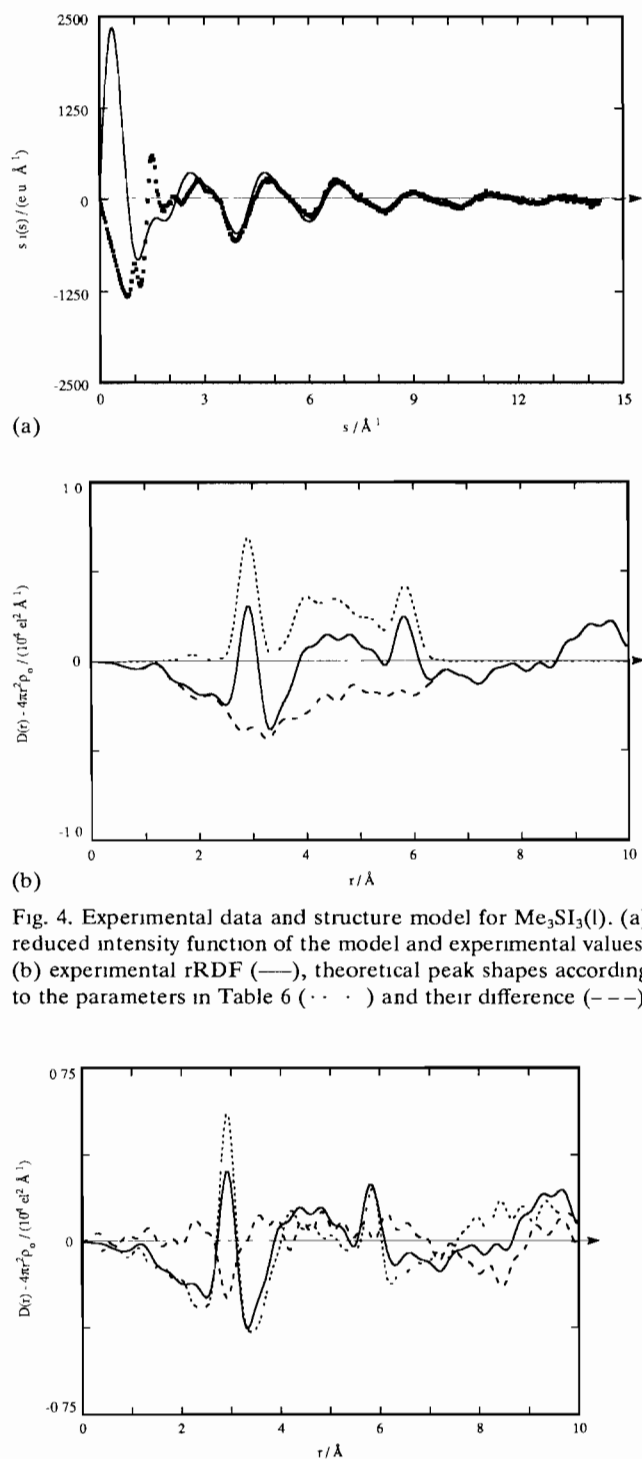


Fig. 4. Experimental data and structure model for $\text{Me}_3\text{SI}_3(\text{l})$. (a) reduced intensity function of the model and experimental values, (b) experimental rRDF (—), theoretical peak shapes according to the parameters in Table 6 (· · ·) and their difference (---).

Fig. 5. Reduced RDFs of molten Me_3SI_3 (—) and Et_3SI_3 (· · ·) and their difference (---)

ions. The results of a least-squares refinement of such a structure model fitted to the reduced intensity function are, together with the corresponding data for $\text{Et}_3\text{SI}_3(\text{l})$, displayed in Table 6.

The I-S interactions between 3.5 and 5.5 Å appear at 3.96, 4.54 and 5.27 Å in molten Me_3SI_3 , as compared

TABLE 6 Calculated distances d , temperature factors b , and number of distances n for the Me_3SI_3 melt Distances for $\text{Et}_3\text{SI}_3(\text{l})$ and $\text{Me}_3\text{SI}_3(\text{s})$ are included for comparison [10] The errors given in brackets correspond to \pm one mean error

Interaction	d (Å)			b (Å ²)	n per I_3^-
	$\text{Et}_3\text{SI}_3(\text{l})$	$\text{Me}_3\text{SI}_3(\text{s})^a$	$\text{Me}_3\text{SI}_3(\text{l})$		
I^1-I^2	2.915(2)	2.915 2.946	2.908(4)	0.0057(5)	1.51(3)
I^1-I^3	5.84(1)	5.86	5.86(1)	0.009(2)	1.0(1)
I^2-S	4.05(1)	3.91	3.96(1)	0.017(2)	3.4(2)
I^1-S	4.57(2)	4.52	4.54(2)	0.025(3)	3.8(2)
I^3-S	5.17(2)	5.25	5.17(3)	0.028(6)	2.6(3)

^aShortest distances to a single triiodide.

to 4.05, 4.57 and 5.17 Å in $\text{Et}_3\text{SI}_3(\text{l})$. The sulfur–triiodide distances are thus virtually identical in the two liquids. The effect of the difference in temperature is expected to be negligible. The slightly shorter S– I^2 distance (**1**) in the methyl compound might indicate a slightly stronger cation–anion interaction.

In Fig. 6 the experimental rRDF of $\text{Me}_3\text{SI}_3(\text{l})$ is displayed together with the rRDF constructed from all atom–atom distances below 6 Å in the corresponding solid. The solid's rRDF was constructed from average atom–atom distances and provided with approximate, realistic temperature factors. The model constructed in this way describes the local structure in $\text{Me}_3\text{SI}_3(\text{l})$ fairly well. The fact that the three S–I distances found in liquid Me_3SI_3 are nearly the same as those to a single triiodide in the solid (Table 6) is conspicuous. However, also other crystallographic S–I distances, even the shortest at 3.81 Å, exist in the solid compound. The predominant feature in the melt seems to be ion-pairing between the sulfonium and triiodide ions. In analogy to the local structure in the solid, a coordination geometry according to that in Fig. 7 can be present also in the liquid. The process of melting imposes structural changes in which distances between species

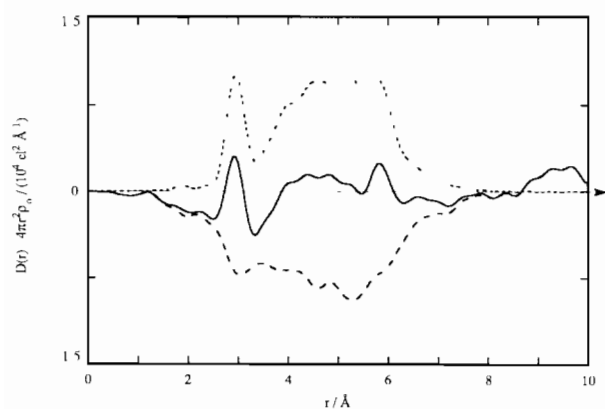


Fig. 6 Experimental rRDF of molten Me_3SI_3 (—) and structure model based on the distances below 6 Å in solid Me_3SI_3 (.....) and their difference (---)

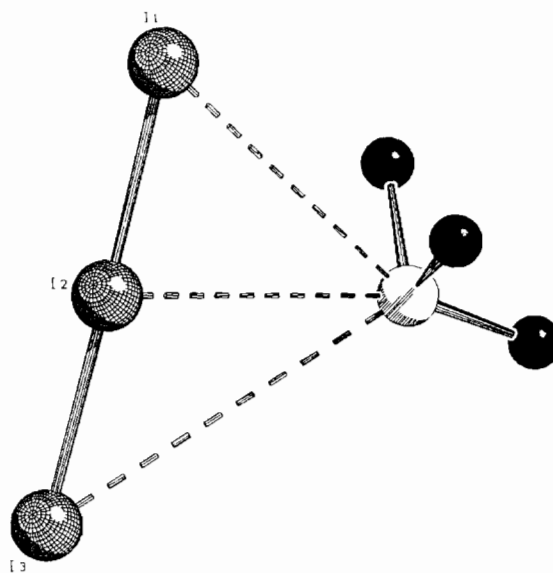


Fig. 7 The triiodide sulfonium coordination, including the orientation of the methyl groups, in Me_3SI_3

of the same charge increase and those of oppositely charged species decrease, together with increased intermolecular mobility. The discrepancy between the local structure in $\text{Me}_3\text{SI}_3(\text{l})$ and $\text{Me}_3\text{SI}_3(\text{s})$, especially about 5 Å, can be attributed to such effects. Whereas all intermolecular distances can be distinctly observed in the solid, they are 'smeared' out for dynamic reasons in the liquid.

The Raman spectra, as shown in Fig. 8, display a difference between solid and molten sulfonium triiodides. The molten methyl and ethyl compounds are, in coherence with the liquid X-ray scattering data, virtually identical and exhibit the typical symmetric stretch vibration from I_3^- as well as strong bands at 145 and 165 cm^{-1} . These bands were previously interpreted in terms of a bond flexibility in the triiodide ions which causes the selection rules to be cancelled and I_2-I^- entities to be observable at the time-scale of Raman spectroscopic measurements. Such a bond flexibility has been theoretically verified by Alvarez and co-workers

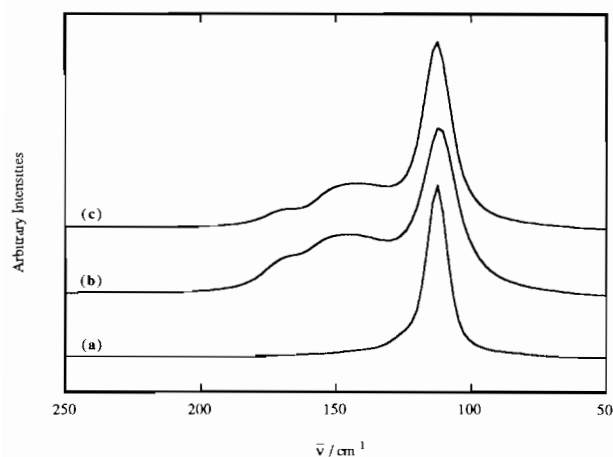


Fig 8. Low-frequency part of the Raman spectra of (a) $\text{Me}_3\text{SI}_3(\text{s})$, (b) $\text{Me}_3\text{SI}_3(\text{l})$, (c) $\text{Et}_3\text{SI}_3(\text{l})$

[18, 19]. In contrast to the spectra of the molten triiodides, solid Me_3SI_3 exhibits a Raman spectrum with one single, slightly asymmetric band at 110 cm^{-1} . This single band indicates that the bond flexibility, as observed in the molten triiodides, is absent in the solid

X-ray absorption spectroscopy, XANES

X-ray absorption spectroscopy, XANES, *i.e.* the spectrum between 10 eV below and 50 eV above the ionization potential, is a sensitive probe of the valency, coordination geometry, symmetry of unoccupied electronic states and the effective charge of a specific element in a molecule or solid compound [20]. Since atoms in similar molecules have similar fine structures in the near-edge region, information about certain molecules can be obtained by comparing XANES spectra of the investigated compounds with those of appropriate reference compounds and using them as fingerprints. The resonances at the K-edge below the ionization potential are assigned to electron transitions from the 1s orbital to unoccupied electronic states below the ionization potential. The so-called shape resonances above the ionization potential, which will not be discussed further, are assigned to multiple scattering of the electron in the continuum [21].

XANES is used in this work to compare bonding relations at the sulfur in liquid and solid sulfonium triiodides. It is known that the absorption maximum is shifted to higher energies with increasing oxidation state of the atom studied. The absorption maxima of the S-K edge at 2472 eV for dialkylsulfides, 2474 eV for trialkylsulfonium iodides, 2475 eV for dimethylsulfoxide, 2479 eV for dimethylsulfone, and higher than 2481 eV for sulfur in sulfate ions, all illustrate this fact [22, 23]. The spectra shown in Fig. 9 of seven different sulfur-containing compounds were used to evaluate the energy-shift difference between the tri-

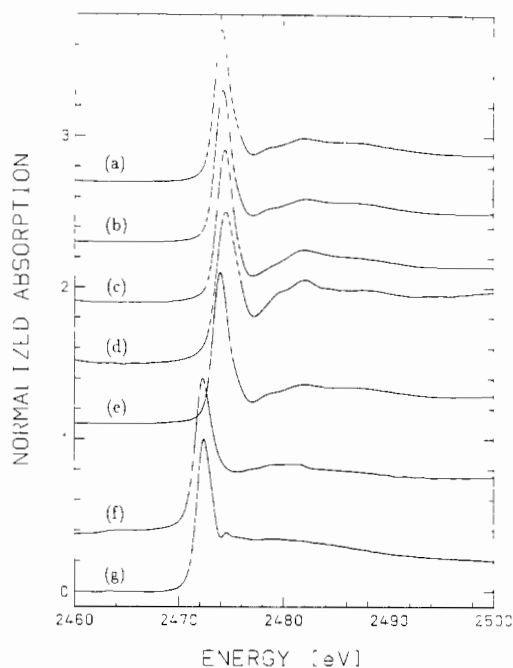


Fig 9. XANES spectra of: (a) $\text{Et}_3\text{SI}_3(\text{l})$, (b) $\text{Et}_3\text{SI}_3(\text{l})$, (c) $\text{Me}_3\text{SI}_3(\text{s})$, (d) $\text{Me}_2\text{S}(\text{s})$, (e) $\text{Et}_2\text{S}\cdot\text{I}_2(\text{l})$, (f) $\text{Bu}_2\text{S}(\text{l})$, (g) $\text{Me}_2\text{S}(\text{l})$

TABLE 7. Energy of the white line of some R_2S , $\text{R}_2\text{S}\cdot\text{I}_2$ and R_3SI_x compounds

Compound	Energy (eV)
$\text{Me}_2\text{S}(\text{l})$	2472.40
$\text{Bu}_2\text{S}(\text{l})$	2472.30
$\text{Et}_2\text{S}\cdot\text{I}_2(\text{l})$	2473.95
$\text{Me}_3\text{SI}(\text{s})$	2474.50
$\text{Me}_3\text{SI}_3(\text{s})$	2474.25
$\text{Et}_3\text{SI}_3(\text{l})$	2474.20
$\text{Et}_3\text{SI}_5(\text{l})$	2474.05

alkylsulfonium polyiodides and the corresponding dialkylsulfides. The reaction of iodine with Et_2S yields a charge-transfer complex $\text{Et}_2\text{S}\cdot\text{I}_2$. The electron-density transfer from sulfur to iodine, as a consequence of the charge-transfer interaction, causes an energy shift of about 1.6 eV compared with the dialkylsulfides (see Table 7). Alkylation of dialkylsulfides by iodoalkane produces trialkylsulfonium iodides. The sulfur oxidation is reflected by an energy shift of about 2 eV. The peak maxima of trimethylsulfonium iodide and various trialkylsulfonium polyiodides are very close in energy. However, there is a tendency to lower energy values (*i.e.* a reduction of the sulfonium sulfur atom) with increasing number of iodine per formula unit. This is probably a polarization effect, due to the increasing anion volume in the series I^- , I_3^- and I_5^- . The chemical bond between (poly-)iodide and the sulfonium cation is thus not purely ionic. Crystallographic data show

that the shortest S–I distances in Me₃SI and Me₃SI₃ are about 0.2 Å shorter than the sum of van der Waals' radii, which may indicate a small covalency of the S–I bond. The induced changes in the XANES absorption maximum of sulfur by exchange of the anion composition shows that the S–K measurements are a sensitive probe of any changes in the electronic environment at the sulfur centre.

There is no significant difference in XANES data between solid Me₃SI₃ and liquid Et₃SI₃ at room temperature. This means that the sulfonium sulfurs are, within experimental error, electronically identical in the two compounds. These results further support previously discussed structural data with respect to the local structure in the solid and liquid trialkylsulfonium triiodides.

Supplementary material

Supplementary data is available from the authors on request.

Acknowledgments

This work has been supported by the Swedish Natural Science Research Council, DFG (Contract no Fu 245) and BMFT (contract no. 055 PDAXI), and the Fonds der chemischen Industrie.

References

- 1 R. Thomas and F.H. Moore, *Acta Crystallogr., Sect B*, **36** (1980) 2869
- 2 T. Bernstein and T.H. Herbstein, *Acta Crystallogr., Sect B*, **24** (1968) 1640
- 3 T. Miggelsen and A. Vos, *Acta Crystallogr.*, **23** (1967) 796
- 4 F.H. Herbstein, M. Kafory, M. Kapon and W. Saenger, *Z. Kristallogr.*, **154** (1981) 11
- 5 S. Christie, R.H. Dubois, R.D. Rogers, P.S. White and M. Zaworotko, *J. Inclusion Phenom. Mol. Recognit. Chem.*, **11** (1991) 103
- 6 K.-F. Tebbe, unpublished results
- 7 J. Runsink, S. Swen-Walstra and T. Miggelsen, *Acta Crystallogr., Sect B*, **28** (1972) 1331
- 8 D.E. Zuccaro and J.D. McCullough, *Z. Kristallogr.*, **112** (1959) 401
- 9 H. Stegemann, A. Rhode, A. Reiche, A. Schmittke and H. Fullbier, *Electrochim. Acta*, **37** (1992) 379
- 10 L.A. Bengtsson, H. Stegemann, B. Holmberg and H. Fullbier, *Mol. Phys.*, **73** (1991) 283.
- 11 L.A. Bengtsson and B. Holmberg, *J. Chem. Soc., Faraday Trans.*, **86** (1991) 354.
- 12 L.A. Bengtsson, *Thesis*, University of Lund, Sweden, 1990
- 13 K.H. Althoff, W. von Drachenfels, A. Dreist, D. Husmann, M. Neckenich, H.-D. Nuhn, W. Schauerer, M. Schillo, F.J. Schittko and C. Wermelskirchen, *Part. Accel.*, **27** (1990) 101.
- 14 M. Lemmonier, O. Collet, C. Depautex, J.M. Esteva and D. Raoux, *Nucl. Instrum. Methods*, **152** (1978) 109
- 15 K.-F. Tebbe, B. Freckmann, M. Horner, W. Hiller and J. Strahle, *Acta Crystallogr., Sect C*, **41** (1985) 660.
- 16 K.-F. Tebbe, H. Stegemann *et al.*, in preparation.
- 17 K.-F. Tebbe, in A.L. Rheingold (ed.), *Homocyclic Rings, Chains and Macromolecules of Main-Group Elements*, Elsevier, Amsterdam, 1977
- 18 J.J. Novoa, F. Mota and S. Alvarez, *J. Phys. Chem.*, **92** (1988) 6561
- 19 S. Alvarez, J. Novoa and F. Mota, *Chem. Phys. Lett.*, **132** (1986) 531.
- 20 A. Bianconi, in D.C. Koningsberger and R. Prins (eds.), *X-ray Absorption*, Wiley, New York, 1988, Ch. 11.
- 21 G. Kuper, R. Chauvistré, J. Hormes, F. Frick, M. Jansen, B. Luer and E. Hartmann, *Chem. Phys.*, **165** (1992) 405.
- 22 K.H. Sze, C.E. Brion, M. Tronc, S. Boduer and A.P. Hitchcock, *Chem. Phys.*, **121** (1988) 279.
- 23 R. Chauvistré and J. Hormes, unpublished results.